Biophysical Chemistry 180–181 (2013) 55–65

Contents lists available at ScienceDirect

Biophysical Chemistry

journal homepage: http://www.elsevier.com/locate/biophyschem

The location of the high- and low-affinity bilirubin-binding sites on serum albumin: Ligand-competition analysis investigated by circular dichroism

Iryna Goncharova [a], Sergey Orlov [a], Marie Urbanová [b,*]

[a] Department of Analytical Chemistry, Institute of Chemical Technology, Prague, Technická 5, 166 28 Prague 6 Czech Republic
[b] Department of Physics and Measurements, Institute of Chemical Technology, Prague, Technická 5, 166 28 Prague 6 Czech Republic

HIGHLIGHTS

- We identified the stereoselectivity of 3 bilirubin-binding sites on serum albumins.
- We identified low- and high-affinity binding sites by ligand-competition experiment.
- We have identified subdomain IIA as a high-affinity bilirubin-binding site.
- Low-affinity bilirubin-binding sites located in subdomains IB and IIIA

GRAPHICAL ABSTRACT

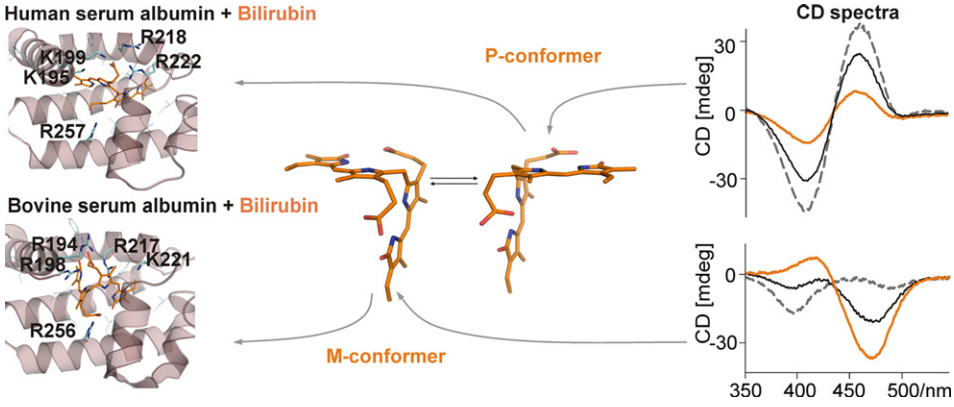

ARTICLE INFO

Article history:
Received 12 April 2013
Received in revised form 28 May 2013
Accepted 4 June 2013
Available online 22 June 2013

Keywords:
Bilirubin
Stereoselectivity
Binding site
Ligand-completion
High affinity
Low affinity

ABSTRACT

The locations of three bilirubin (BR)-binding sites with different affinities were identified as subdomains IB, IIA and IIIA for five mammalian serum albumins (SAs): human (HSA), bovine (BSA), rat, (RSA), rabbit (RbSA) and sheep (SSA). The stereoselectivity of a high-affinity BR-binding site was identified in the BR/SA = 1/1 system by circular dichroism (CD) spectroscopy, the sites with low affinity to BR were analyzed using difference CD. Site-specific ligand-competition experiments with ibuprofen (marker for subdomain IIIA) and hemin (marker for subdomain IB) did not reveal any changes for the BR/SA = 1/1 system and showed a decrease of the bound BR at BR/SA = 3/1. Both sites were identified as sites with low affinity to BR. The correlation between stereoselectivity and the arrangement of Arg-Lys residues indicated similarity between the BR-binding sites in subdomain IIIA for all of the SAs studied. Subdomain IB in HSA, BSA, SSA and RbSA has P-stereoselectivity while in RSA it has M-selectivity toward BR. A ligand-competition experiment with gossypol shows a decrease of the CD signal of bound BR for the BR/SA = 1/1 system as well as for BR/SA = 3/1. Subdomain IIA was assigned as a high-affinity BR-binding site. The P-stereoselectivity of this site in HSA (and RSA, RbSA) was caused by the right-hand localization of

Abbreviations: BR, bilirubin; BSA, bovine serum albumin; CD, circular dichroism; dCD, difference circular dichroism; GS, gossypol; HSA, human serum albumin; Ibf, ibuprofen; PSB, phosphate saline buffer; RbSA, rabbit serum albumin; RSA, rat serum albumin; SA, serum albumin; SSA, sheep serum albumin.

* Corresponding author at: Marie Urbanová, Department of Physics and Measurements, Institute of Chemical Technology, Prague, Technická 5, 166 28 Prague 6, Czech Republic. Tel.: +420 22044 3036; fax: +420 22044 3443.
E-mail addresses: iryna.goncharova@vscht.cz, sergey.orlov@vscht.cz (I. Goncharova), marie.urbanova@vscht.cz (M. Urbanová).

0301-4622/$ – see front matter
http://dx.doi.org/10.1016/j.bpc.2013.06.004

charged residues R257/R218–R222, whereas the left-hand orientation of R257/R218–R199 led to the M-stereoselectivity of the primary binding site in BSA (and SSA).

1. Introduction

Serum albumin (SA) is the most abundant protein in the circulatory system of mammals. It is a single, nonglycosylated polypeptide which is organized in the form of a heart-shaped protein having about 67% α-helix but no β-sheet [1,2]. The protein has three homologous domains I–III, each of which is comprised of two subdomains, A and B, which possess common structural elements. SAs from different mammals have a high homology in amino-acid constitutions [2]. Due to its high concentration in plasma (around 0.6 mM), SA makes a major contribution to the colloid osmotic pressure of plasma and serves as a significant reservoir for the signaling molecules. In the circulation, however, its principal functions are reversible binding and the transport of a variety of endogenous substances including nutrients, hormones, metal ions, drugs and waste products [2–6].

One of these transported substances is bilirubin (BR). In present-day biochemistry, this breakdown product of heme has been associated with both cytotoxic and antioxidant properties in mammals [7]. Although BR is a dicarboxylic acid and contains several polar functional groups, it is highly lipophilic and poorly soluble in water. This is caused by the unique 3D structure of the pigment fixed by the frame of intramolecular hydrogen bonds (Fig. 1). BR is a member of the so-called linear tetrapyrrole family, but it is not linear. In solution and solid states, the pigment is a mixture of two isoenergetic M- and P-helical conformers [8]. The adopted helical conformation is shaped like ridge tiles and stabilized by the frame of intramolecular hydrogen bonds between pyrrole/lactam functions and propionic carboxyl (or carboxylate) groups. In a ridge-tile-like chiral structure, an exciton coupling between two dipyrrinone chromophores splits the excited state of BR into two energy levels, which leads to bisignate CD signals (Fig. 1). When the orientation of the transition dipoles of the two dipyrrinone chromophores adopts an M-helical structure, the negative and positive CD signals appear at the longer and shorter wavelengths, respectively, forming a so-called negative couplet. A positive couplet is observed for a P-helical structure of BR [8]. The ridge-tile conformation is the only one that has been observed in the crystals of BR and its carboxylate salts [9]. The conformations are relatively flexible and in the complexes, the pigment may adopt more closed or open conformations, but the hydrogen bonding network is never completely broken. The chirality depends on their backbone shape of the conformations, and circular dichroism (CD) is the perfect method to monitor and study these complexes [8,10–13]. Unbound pigment racemizes easily and its solution is not optically active. It is the chromophore perturbation in the complex with albumin that makes BR optically active [10].

Albumin solubilizes BR and acts as a buffer preventing the transfer of BR from the blood to the tissues [14]. The binding occurs at only a few ligand-binding sites: one primary (K_a ~ 10^8 M^{-1}) and two secondary [15–18]. The structural information on HSA–drug interactions has emerged only very recently and in a rather piecemeal fashion; most drug-binding studies have therefore adopted a ligand-based approach to the problem [4]. The accumulated data can be used to

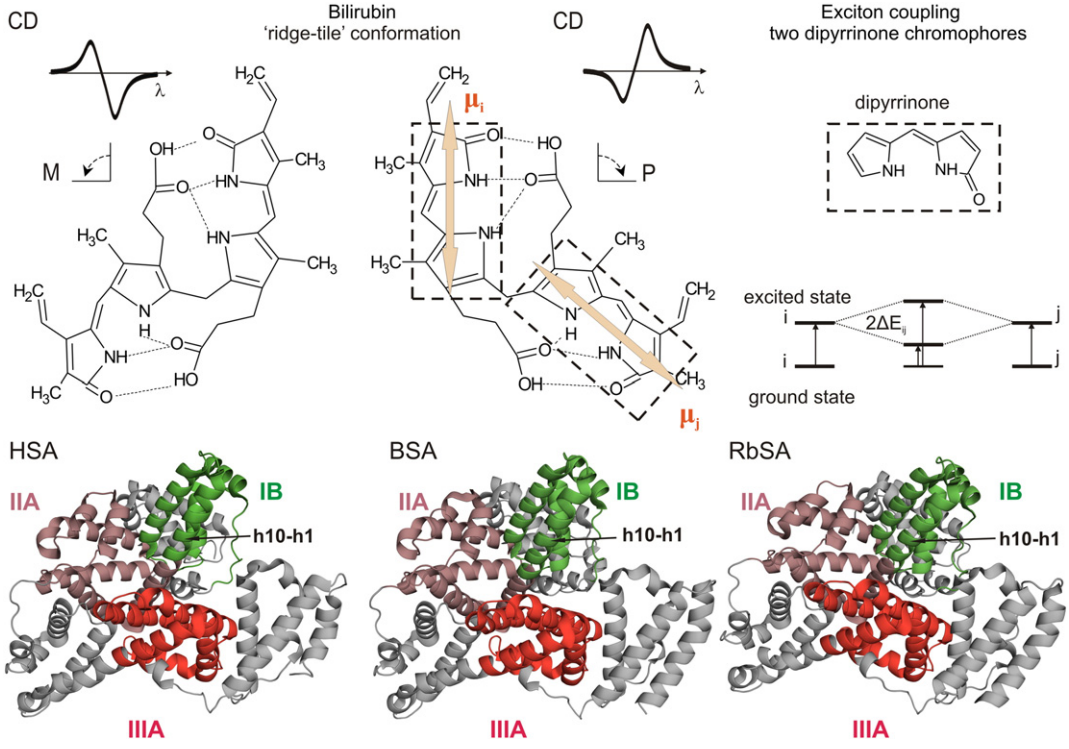

Fig. 1. The interconverting, intramolecularly hydrogen-bonded enantiomeric ridge-tile P- and M-conformers of bilirubin IX alpha (BR). The relative orientations of the electric-dipole transition moments of the two dipyrrinone units are shown by the orange lines. Exciton coupling leads to the energy-level splitting and the bisigned circular dichroism (CD) couplet shown schematically for P- and M-conformers. The ribbon models of human (HSA, PDB: 2VUE), bovine (BSA, PDB: 3V03) and rabbit (RbSA, PDB: 3V09) serum albumins are shown. The proposed binding sites are colored in green (subdomain IB), violet (IIA) and red (IIIA). The figures have been generated using PyMOL (http://www.pymol.org/).

develop quantitative structure–activity relationships for albumin binding.

In 2008, BR was found to be bound in subdomain IB in human SA (HSA) [19]. Nevertheless, crystallography showed the M-conformation of the pigment; this was in disagreement with the proposed P-conformation of BR in complex with HSA, which had also been proven by calculations [10]. The Z,E stereo conformation of the pigment, revealed by crystallographic analysis, was also unexpected. In solution, the Z,E form was found to be much less frequent than the main Z,Z form of the pigment [20]. Until now, the location of the primary BR-binding site is still under discussion.

Crystallographic studies have yielded a highly detailed map of serum-albumin binding sites, but they cannot provide information on affinities. On the other hand, CD spectroscopy is well suited to providing complementary data on relative affinities that can be correlated with structural data. Since the BR–SA complexes are optically active, CD spectroscopy is a widespread technique for the structural characterization of BR complexes [8,10–13,21]. CD spectroscopy has revealed the interference of BR binding sites with some drugs and other ligands [2,20,22,23]. Previous work [13] using bovine serum albumin (BSA) and HSA has shown that the progressive titration of albumin with BR reveals changes in the spectra associated with three evident binding sites on the protein. Additionally, the intensity and shape of these signals are dependent on the molar ratio of BR/SA and imply the presence of three binding sites with different stereoselectivity of the bound pigment. The CD studies of BR interactions with proteolytic fragments of HSA have revealed that a high-affinity site is located in domain IIA while the secondary sites reside somewhere within the fragment consisting of subdomains IB and IIIA.

In this study, chiroptical properties of the three binding sites of mammalian SAs from five different species (human, cow, sheep, rat and rabbit) were investigated in complexes with BR using CD spectroscopy. We now aim to make a more precise assignment of the stereoselectivity of the binding sites that can be linked to a specific BR-binding site location. Additionally, here we extend this method to complete the assignment of the relative affinities of the pigment sites on the five studied SAs by using drugs and other small-molecule ligands as specific markers for BR-binding sites. This approach exploited the recent crystallographic data that revealed the precise binding locations of these ligands and allowed us to extend in a novel way the well-established method of using the marker ligands to probe binding to the protein. Our results provide the first complete correlation of CD data and propose the location of the primary binding site with high affinity and the secondary ones for BR on the albumins studied.

Each site of the albumins was analyzed by a combination of the bound BR conformation obtained using CD spectroscopy, the crystallographic data of the spatial domain structure, amino-acid constitution, and the competition effect of the selected marker ligands (hemin, gossypol and ibuprofen).

2. Materials and methods

2.1. Preparation of the samples

The bovine (BSA; A7030), human (HSA; A3782), rat (RSA; A6414), sheep (SSA; A6289) and rabbit (RbSA; A9437, A0764) albumins were purchased from Sigma/Aldrich (USA) with the high purity, globulin and fatty-acid free Cohn fraction V and were used without further purification. The stock solutions of the proteins were prepared by dissolving 5 mg of albumin in 1 mL of 0.1 M phosphate saline buffer (PSB, 0.14 M NaCl, 0.0027 M KCl, 0.010 M PO_4^{3-}, pH 7.4 at 23 °C). Protein concentrations were determined spectrophotometrically by UV-spectroscopy using the absorption at a wavelength of 280 nm. The values of the molar absorption coefficient at 280 nm for HSA ($\varepsilon_{280} = 35{,}500\ M^{-1}\ cm^{-1}$) and BSA ($\varepsilon_{280} = 43{,}300\ M^{-1}\ cm^{-1}$) were obtained from [24]; these values for RSA ($\varepsilon_{280} = 39{,}000\ M^{-1}\ cm^{-1}$), SSA ($\varepsilon_{280} = 43{,}300\ M^{-1}\ cm^{-1}$) and RbSA ($\varepsilon_{280} = 43{,}500\ M^{-1}\ cm^{-1}$) were calculated according to [24].

Z,Z-bilirubin-IX alpha (BR; 635-65-4) from Frontier Scientific was used for salt preparation. Sodium hydroxide and hydrochloric acid were supplied by Sigma/Aldrich (USA) and were used as received. The disodium salt of the pigment was prepared by the freeze-drying method [12]. Only freshly prepared salt was used for the experiments. Doubly-distilled water was utilized as a solvent for the stock solutions of BR ($c(BR) = 3 \cdot 10^{-3}$ mol L^{-1} in 0.01 M NaOH).

The working solutions of the SA–BR complexes were prepared from the protein stock solution and a stock solution of BR by dilution in PSB. The SA concentration $c(SA) = 1.5 \cdot 10^{-5}$ mol L^{-1} was kept constant for all spectral measurements. The BR concentrations were determined by the desired BR/SA ratio and lay in the interval of $1.5 \cdot 10^{-5}$–$4.5 \cdot 10^{-5}$ mol L^{-1}. This interval of the BR concentration was used as optimal to ensure the significant occupancy of all binding sites and to minimize the pigment self-assembly, binding of its aggregates or sedimentation.

2.2. Ligand-competition experiments

The stock solutions of the marker ligands hemin (16009-13-5, Frontier Scientific), ibuprofen (Ibf; I14892, Fluka) and gossypol (GS; 303-45-7, Santa Cruz Biotechnology) were prepared at a concentration of $3 \cdot 10^{-4}$ mol L^{-1}. The structures of the ligands used are shown in Fig. S1.

Complexes with SA were obtained by the addition of the stock solutions of BR and/or marker ligand to protein solutions. SA concentration was kept constant in all of the studied solutions ($c(SA) = 1.5 \cdot 10^{-5}$ mol L^{-1}), and the final molar ratios BR:SA/ligand were 1/1/1 and 3/1/1 or 3/1/3 for BR/SA/Ibf. In the first series, the complex of SA and marker ligand was prepared at the molar ratio SA/ligand = 1/1, after which BR was added to the system. In the second series, the ligand was added to the previously prepared BR complex. The third series was prepared by a simultaneous addition of the stock solutions of BR and ligand to the SA solution. The relative differences between the measured CD intensities in the three mentioned series were less than 5%. All of the measurements were performed 15 min after the preparation.

2.3. CD measurements

The CD spectra were recorded on a Jasco J-810 spectrometer at 23 °C using a quartz cell with a path length of 1 and 0.1 cm for spectral regions of 300–550 and 190–250 nm, respectively. The conditions of the measurement included a scanning speed of 100 nm min^{-1}, a bandwidth of 1 nm, the standard sensitivity setting, an integration time of 2 s for each spectral point and 3 accumulations. The spectrometer was flashed by nitrogen and the measured solutions in cuvettes were kept under nitrogen atmosphere.

2.4. Molecular docking

The molecular docking of BR to HSA, BSA and RbSA was performed using the 3D crystal structure of these proteins (PDB codes 2VUE, 3V03 and 3V09, respectively) obtained from the Protein Data Bank [19,25]. The ionizable residues were set to their pH 7.4 protonation states; the His, Arg and Lys were protonated while those of Asp and Glu were deprotonated. During the minimization, only the torsion angles in the side chains were modified; all the other properties including bond lengths and backbone-atom positions were kept fixed. The AutoDock Vina v.1.0.2 plugin was used for all dockings in this study [26]. The docking parameters for AutoDock Vina were kept to their default values. The docking results were ranked by the binding free energy. The binding modes with the lowest binding free energy and the most cluster members were chosen for the optimum docking

conformation. The binding results were illustrated using the PyMOL Molecular Graphics System Version 1.5 (Schrödinger, LLC).

3. Results and discussions

3.1. Bilirubin binding to serum albumins

The stereoselectivity of BR binding to SA makes it possible to employ advantageously CD spectroscopy for the characterization of the bound BR. In our previous study [13], we characterized three proposed independent binding sites of BR in defatted human and bovine SAs by the CD spectra, one primary site with high affinity and two secondary sites with lower affinity.

Fig. 2 shows the results of the titration of human (HSA), bovine (BSA), sheep (SSA), rat (RSA) and rabbit (RbSA) SAs by BR in PSB at pH 7.4. The homology of the studied albumins, expressed as the amino-acid sequence identity, is higher than 75% and the crystallographic structures of HSA, BSA and RbSA are known. The complexes of BR and the studied SAs exhibited distinctly different CD spectra, which strongly depended on the molar ratio BR/SA. According to the observed data, the BR–SA complexes were divided into three groups. To eliminate the presence of bound ligands in the actual SA samples, the CD spectra of SAs without BR measured under the same conditions were checked and are shown in Fig. S2 (Supplementary materials).

The first type of the CD spectra was observed for BR with HSA and had already been described in detail before [11]. The complex formed at the BR/HSA = 1/1 was characterized by the induced CD positive couplet located at 460(+)/410(−) nm, which is characteristic for the bound P-conformer of BR. In the complexes with HSA, BR has a long-wavelength electronic transition with an absorption maximum at 475 nm, which is red-shifted as compared to the unbound pigment in solution (440 nm). A more open conformation of the bound BR was proposed and was supported by energy calculations [10,21]. The titration of HSA by BR caused an increase of the CD positive-couplet intensity, which indicated the chiral bonding of titrated BR. The maximum capacity was achieved at the ratio BR/HSA = 3/1. The addition of further BR caused only minor changes in the CD spectrum, which reflected that the additional BR molecules did not bind enantioselectively. The dependence of exciton magnitude (e.g. the difference between the intensity of the positive and negative components of the exciton couplet) on the BR/HSA ratio in the interval from 1 to 5 also indicated that the three molecules of BR were enantioselectively bound to a SA molecule (see the upper panel of Fig. 2). Because of the difference of three orders of magnitude in the association constants between the primary site and the secondary ones, a preferential participation of BR in the primary binding site was supposed [2]. Therefore, each CD spectrum for each BR/SA ratio contains the spectrum of the BR complex bound in the primary site. Then, the difference spectrum (indicated as dCD in the figure) obtained by the subtraction of the BR/SA = 1/1 spectrum from that

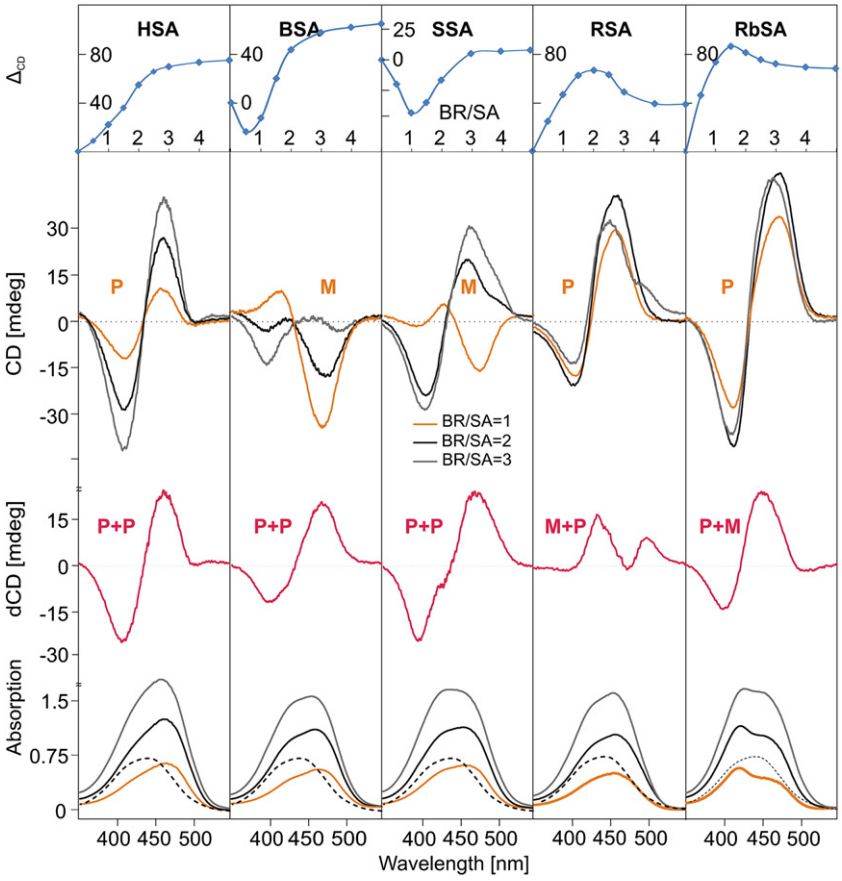

Fig. 2. The CD and absorption spectra of BR complexes with human (HSA), bovine (BSA), sheep (SSA), rat (RSA) and rabbit (RbSA) serum albumins (c(SA) = 1.5 · 10^{-5} mol L^{-1}) at the molar ratios BR/SA = 1; 2; and 3 (orange, black, thick gray); the absorption of BR without chiral agent at 1.5 · 10^{-5} mol L^{-1} (dotted lines). The CD spectra of the BR–SA complexes at the molar ratio BR/SA = 1 are a stereoselective reflection of the primary binding site (orange); the ones at the molar ratio BR/SA = 2 and 3 reflect all the binding sites (black and gray); the difference between the CD spectra of the molar ratios BR/SA = 3 and BR/SA = 1 (dCD, red) reflects the BR enantioselective binding to the secondary binding sites. The difference between the intensity of the long- and short-wavelength components of the exciton couplet (Δ_{CD}) as a function of the BR/SA ratio (the upper panel) demonstrates different stereorecognition of the SAs studied.

measured for BR/SA = 3/1 reflected the enantioselective bindings in the secondary sites. Both the observed spectrum for the BR–HSA complexes for BR/SA = 1/1 and the difference for BR–HSA were typical for the P-conformer of the bound BR, therefore the bound BR in both the primary site and the secondary ones was formed by the P-conformer.

Considering the spectral features of BR titration, the second group comprised BSA and SSA. The addition of the first equivalent of the pigment (BR/SA = 1/1) for this second group induced a negative CD couplet located at 476(−)/420(+) nm for the BR bound in the high-affinity binding site of BSA and SSA, opposite to that observed for HSA. The binding of the M-conformer in the primary site concurred with these observations. However, further addition of BR caused a decrease in the both patterns of the CD couplet followed by the inversion of the signal, which culminated at the point when the molar ratio was BR/SA = 3/1. The difference spectra show that the opposite P-conformer of the pigment was bound to the secondary sites of BSA and SSA.

On the basis of the spectral features presented in Fig. 2, the third group consisted of BR complexes with RbSA and RSA. Up to the molar ratio BR/SA = 2/1, the gradual increase of the positive CD couplet at 450(+)/410(−) nm was observed. According to that, the primary binding sites of RbSA and RSA selectively bind BR as a P-conformer. The CD changes in the system above the ratio BR/SA = 2/1 were not gradual and as pronounced as in the previous two groups of SAs. Further BR addition caused only a slight decrease of CD band intensities. We suppose the existence of at least one binding site with low affinity. The binding of the P-conformer in the secondary site concurred with the observed difference spectra. The CD results suggested that both RbSA and RSA bound the first and second BR molecules as P-conformers. Still further BR addition to RSA caused a slight decrease of CD band intensities. We cannot exclude that the binding of the second and third BRs was directed at the preferred secondary site. Rather, the second added equivalent was distributed between both of them. If these sites preferred the same pigment conformer, the resulting changes in the CD spectra would reveal a progressive increase of the characteristic CD signal, like it was observed for the studied proteins in the two previous groups. In the case of RSA, however, the secondary sites have the opposite stereoselectivity for BR binding, the second and third bound BR molecules evoke the opposite CD signals and the resulting CD spectrum has shown a minor decrease (for RSA), depending on the relative affinity of the secondary sites. This proposition has been proven by a competition experiment and will be discussed later. In the case of RbSA, BR may also have more than one secondary binding site; nevertheless, their coexistence together, like their stereoselectivity, cannot be proven by CD definitely.

Summarizing the listed results, the CD spectra of the BR–SA complexes shown in Fig. 2 reflected the chiroptical properties of the pigments bound in primary and secondary binding sites as well as the similarities and differences in the binding-site structures in each group of the albumins studied. The stereoselectivity of the binding sites for each mammalian species is presented in Table 1.

Table 1
The stereoselectivity of the binding sites on the studied mammalian serum albumins toward BR.

	HSA	BSA	SSA	RSA	RbSA
Primary binding site	P	M	M	P	P
Secondary binding sites	P + P	P + P	P + P	P + M	P

3.2. The location and structure of the serum-albumin binding sites

The solved crystal structures, which are known for three of the studied SAs (HSA, PDB 2VUE; BSA, PDB 3V03 and RbSA, PDB 3V09) [19,25], are shown in Fig. 1. Their spatial conformations are similar, which corresponds to their high homology, expressed by the amino-acid sequence identity (near 75%) [2]. Therefore, we propose the same location of the binding sites for all of the SAs studied. At the same time, our CD analysis presented in Fig. 2 clearly documents the differences in the stereoselective properties of the binding sites, which obviously correlate with the residue composition of the binding sites. Considering the fact that the location of the primary site is still under debate, all potential sites were analyzed based on a combination of several properties — amino-acid constitution, stereoselectivity, hydrogen-bonding potential and the spatial organization of the binding sites. As a complementary method, we used the marker ligands, which are known to bind in specific albumin sites. The impact of these ligands on the chiroptical properties of the BR–SA was used to identify the BR binding sites.

The principal functions of SAs are reversible binding and the transport of variety endogenous substances including nutrients, hormones, metal ions, and waste products. Many commonly used drugs with acidic or electronegative features also bind to SA, usually at one of two primary sites (1 and 2), located in subdomains IIA and IIIA, respectively [1,2]. Site 1 (subdomain IIA) mainly binds hydrophobic, bulky, heterocyclic molecules with a centrally located negative charge (e.g. warfarin, sulfonamides); drug site 2 (subdomain IIIA) binds aromatic carboxylic acids with a negative charge at an end of the molecule distal from the remaining hydrophobic structure (e.g. diazepam, ibuprofen). BR is able to bind to both of these sites in the SA structure, because it is a lipophilic compound with four aromatic rings in its structure and at the same time has two negatively charged carboxyl groups. Two of the discussed sites are classified as BR-binding sites with high and low affinities. Simultaneously, we should note that electrostatic interactions mainly contribute to the BR–SA complex formation, specifically the positively charged residues of the binding sites are critical in providing the free energy for the SA–BR binding as was proven by both spectroscopic studies with BR ethers and the difference calorimetric method [8,10,15,16,20]. At the same time, aromatic residues help stabilize the pigment conformation in this complex.

Most authors agree with the anticipation of subdomain IIA (residues 190–292) as the primary binding site for BR [1,2,5,11,20,27–29]; nevertheless, based on the latest X-ray data for the BR–HSA complex, it has been determined that a possible location of the primary binding site is the subdomain IB (residues 117–190) [19], a neighbor to IIA. Mutation experiments have not been able to exclude any of these propositions; the provable differences in BR binding on native and mutated SAs have been mostly associated with the residues placed between these domains [20,22,28].

Because of the intrinsic sensitivity of CD to the structure, we assumed that the main reason for the observed CD signal diversity was the structural and compositional dissimilarity of the binding sites. An analysis of the 3D structure of the proposed binding sites, their stereoselectivity and a comparison of their amino-acid situation led us to suppose that only particular residues were involved in the complex formation. A potential limitation of this proposition is that we compare the solution structure reflected by CD spectroscopy while using the knowledge obtained by crystallographic studies.

To identify the possible BR-binding site affinity and location in correlation with CD data, we employed a complementary methodology of adding competitive ligands which are able to site-specifically displace the BR from the studied proteins, and this competition is site-specific. This approach is possible, because recent crystallographic analyses of drug or small-molecule binding to HSA provide a database of structures with the binding locations of different compounds and show that it is possible to find the appropriate ligand that is able to compete with a BR molecule for binding to a specific site [1–5]. In competition experiments, we used ligands that selectively bind to only one or two primary sites on the protein at the locations that overlap with one of the proposed BR-binding sites; specifically, the natural ligand hemin binds to subdomain IB, which overlaps with one of the proposed BR sites [19]; the drugs gossypol and ibuprofen were then used as markers for the binding sites located in subdomains IIA [30] and IIIA [2,4], respectively. The structures of the ligands used are shown in Fig. S1.

3.2.1. Subdomain IB

The first of the proposed BR binding sites is subdomain IB (Fig. 3). According to the crystallographic data for the BR–HSA complex, the central hydrophobic channel in the L-shaped pocket of subdomain IB was formed by four helices (h7–h10) [3,19]. The polypeptide that connects this subdomain with subdomain IA (residues 110–119) makes a "strap". The formation of salt bridges is possible with a "focal" residue of the site, Arg-186, and one of the charged residues on the polypeptide "strap", Arg-117, for HSA, which lies at the entrance to the binding cleft. The pigment is situated in the deepest part of the channel and makes close contacts with the apolar side chains of the residues from helices h8–h10 (Ile-142, Phe-149, Leu-154, Phe-157, Gly-189). It has been proposed that the binding is accompanied by only minor conformational changes of the other side chains lining the binding site [19]. The carbonyl oxygen of the lactam ring in the pigment is also fixed by the hydrogen bonds with the side chain of Tyr-138 and/or Tyr-161. The differences in the structure and organization of this binding site for the other studied SAs are discussed in the SI.

To identify the affinity of this binding site, a competition experiment with hemin was performed. Hemin, a porphyrin molecule with a coordinated iron atom, is a large planar ligand that selectively binds within subdomain IB [19]. BR- and hemin-binding sites are crossed over; both ligands compete for the location in the pocket and the same binding residues. Hemin has a binding constant comparable to BR ($K_a = 1.1 \cdot 10^8\ M^{-1}$) and was proposed to displace BR from this binding site [2]. The crystal structure of the hemin–HSA complex is known; hemin binds within a narrow cavity in the subdomain IB of HSA with an axial coordination of Tyr-161 and electrostatic interactions between the porphyrin and the basic amino-acid residues in the vicinity (Lys-190, Arg-186 His-146, Arg-114, Arg-117) [19].

Fig. 4 shows the CD spectra which compare BR–SA and BR–hemin–SA for the SAs studied. The interaction of SA with BR and hemin is proved by absorption spectra: a typical spectrum for bound BR was observed and the band at 388 nm for unbound hemin was red-shifted to 402 nm for hemin bound to HSA (see SI, Fig. S3). Hemin is intrinsically optically inactive; when bound to HSA, an induced negative CD band centered at 402 nm appears. Unlike HSA, other mammalian SAs induced only a weak negative CD band of bound hemin. However, the absorption spectra typical for bound hemin proved the hemin binding on SAs.

As documented in Fig. 4, the CD signs of the BR–SA pattern for the BR/SA = 1/1 are the same for the system with and without hemin. The observed CD spectra are the results of the superposition of the CD spectra of both bound hemin and BR. Only a minor decrease of the positive-sign pattern was observed for the BR–BSA and BR–RSA complexes in the presence of hemin. Our experiment suggests that hemin and BR bind independently on all the studied proteins for BR/SA = 1/1. The primary binding sites of these compounds do not cross over; subdomain IB is not a high-affinity BR-binding site.

To test our initial identification of this subdomain as one of the sites with low affinity, we studied the system where all three sites were occupied with BR. In the system with the molar ratio BR/SA = 3/1, the observed differences were associated with competition in secondary binding sites. The presence of hemin in the solution for the competition experiment led to a decrease of the CD intensity of BR stereoselectively bound to SAs. The results suggest that hemin binding to SA overlapped with one of the secondary binding sites. The difference spectra obtained by the subtraction of the spectra when hemin was present (BR/SA/hemin = 3/1/1) and the spectrum of hemin bound to SA from the spectra without hemin (BR/SA = 3/1) showed a characteristic positive couplet for all SAs except for RSA. This documented the blocking of one secondary site with the preference binding of BR as a P-conformer for all SAs studied except for RSA, where the difference spectra showed the blocking of the site with the opposite stereoselectivity. This fact is in accordance with our proposition that the arrangement of the charged residues correlates with the stereoselectivity of the binding site. A simulation of the BR binding to subdomain IB of HSA, BSA and RbSA agrees with the proposed preference of the P-conformer of BR. The BR molecule is oriented along the L-cavity of the subdomain with the propionic group arranged in the way of the salt-bridge formation with charged residues

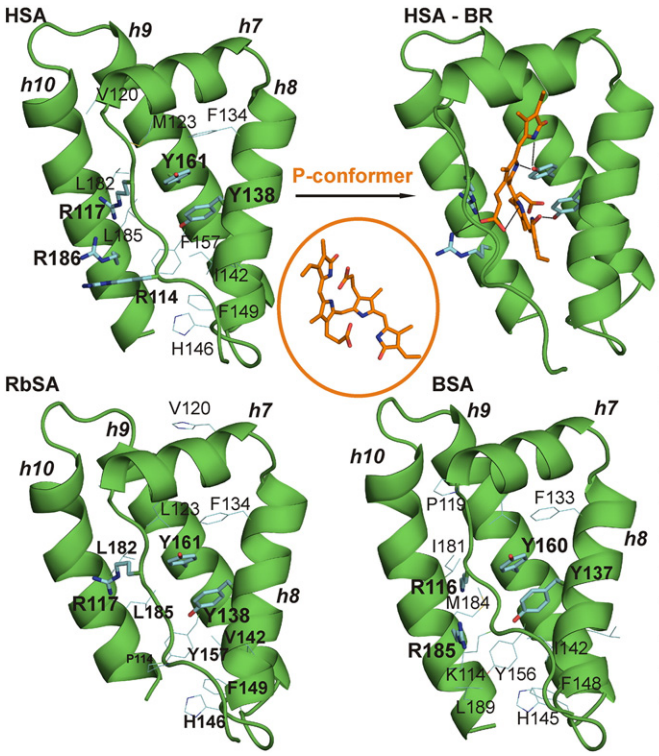

Residue	Albumin HSA	RbSA	RSA	Residue	Albumin BSA	SSA
114	R	P	P	114	K	K
117	R	R	R	116	K	K
120	V	A	A	119	P	P
123	M	L	M	122	L	L
128	H	H	Q	127	K	K
134	F	F	F	133	F	F
135	L	F	F	134	W	W
138	Y	Y	Y	137	Y	Y
142	I	V	V	141	I	V
146	H	H	H	145	H	H
149	F	F	F	148	F	F
154	L	L	L	153	L	L
157	F	Y	Y	156	Y	Y
161	Y	Y	Y	160	Y	Y
185	L	L	V	184	M	M
186	R	E	K	185	R	R
189	G	K	K	188	K	K

Fig. 3. The model of BR binding in subdomain IB for human (HSA), bovine (BSA) and rabbit (RbSA) serum albumins and the amino-acid sequences for human (HSA), rabbit (RbSA), rat (RSA), bovine (BSA) and sheep (SSA) serum albumins.

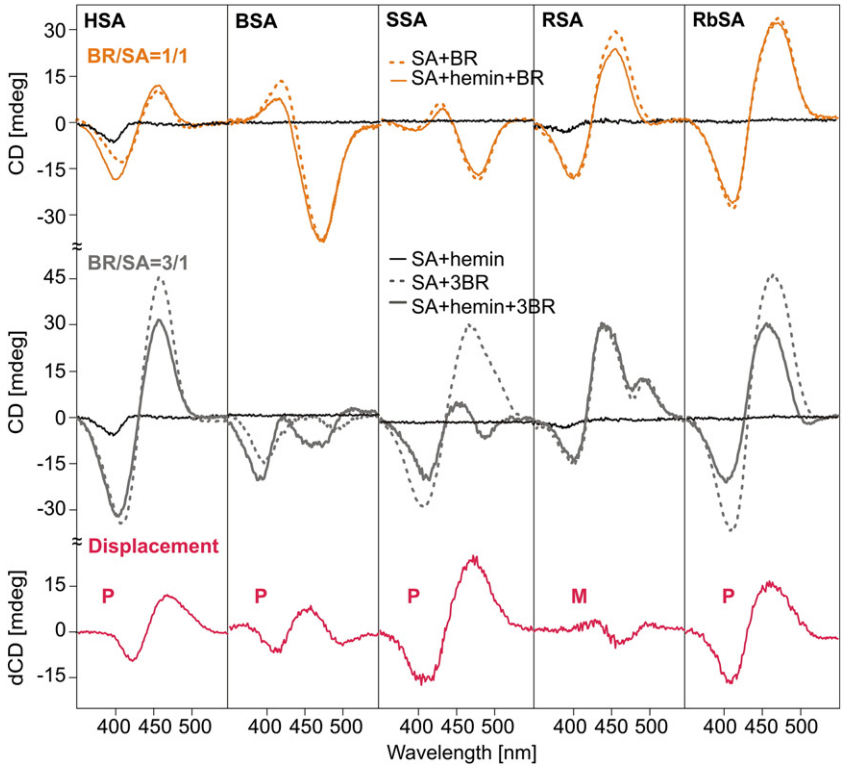

Fig. 4. The CD spectra of the BR complexes with human (HSA), bovine (BSA), sheep (SSA), rat (RSA) and rabbit (RbSA) serum albumins at the molar ratios BR/SA = 1/1 (orange) and BR/SA = 3/1 (gray) in the presence of hemin at the molar ratio BR/SA/hemin = 3/1/1 (full lines) and without hemin (broken lines). The CD spectra of the SA–hemin complexes at the molar ratio SA/hemin = 1/1 are shown as black lines, the difference spectra dCD (red) were obtained when both BR/SA/hemin = 3/1/1 and SA/hemin = 1/1 were subtracted from BR/SA = 3/1 and reflect the stereoselectivity of the BR-binding site blocked by hemin.

lying near the entrance (Arg and Lys at positions 185–186 and 116–117). Unlike the other SAs, RSA has Lys-186, which has determined the stereoselectivity of this site. The M-conformer of the pigment is more preferred in this case.

Combining the results of the displacement experiment and the specified stereoselectivity of the primary binding site, we conclude that subdomain IB is not a high-affinity site; it is one of the secondary sites for BR binding.

3.2.2. Subdomain IIA

The next possible binding site is located along the h10–h1 helix. Whereas the top of the helix is involved in the binding within subdomain IB (residues 177–195), the binding site within subdomain IIA involves its consequential part of the helix (195–205) [1,4,31] (Fig. 1). Many authors have proposed subdomain IIA as the primary binding site for BR, and this consideration is in agreement with mutation experiments [20,28] and the proteolytic fragments of HSA and BSA [27,29,32]. An analysis of the published data concerning BR binding to albumins with modified and mutated residues in this region has led to the conclusion that BR was bound along the h10 (IB)–h1 (IIA) helix of residues 177–205. The hydrophobic cavity of the IIA domain is hence a potential primary binding site. The crucial residues were found to be Lys-199 and/or Arg-222, located close to the center of the binding site.

From a number of studies, it has been known that some drugs displace BR from its primary binding site [2,33]. GS was used as a marker for drug site I (subdomain IIA), which overlaps with the BR site in our competing experiment. GS has only one binding site on the HSA structure and the binding constant $K_a = 1.8 \cdot 10^8\ M^{-1}$ [2,30].

We can hypothesize that under these conditions the displaced BR was partly able to migrate to one of the secondary sites when they were unoccupied, and the resultant signal was the superposition of the spectra originating from the BR bound in primary and secondary sites. Accepting this proposition, the changes in the CD spectra were studied in two systems, BR/HSA = 1/1 and 3/1, in the presence of GS (Fig. 5). For BR/HSA = 1/1 in the presence of GS, a relative decrease of the CD intensity was 45% as compared to the same without GS. If we realize that the secondary sites of HSA prefer the binding of the same P-conformer as the primary site, we can interpret this observation as partial binding of BR, replaced by GS, into secondary sites of the same stereoselectivity. For BR/HSA = 3/1, a 42% decrease of the CD signal was observed in the presence of GS, which documented the decrease of the ability of BR binding by HSA from three to two binding sites; however, it is still the question of the affinity of the blocked site, because both the primary and secondary binding sites of HSA have the same stereoselectivity. Simultaneously, in the second group of the SAs studied, in BSA and SSA, the presence of GS caused an inversion of the CD signal as a result of the excess of the P-conformation of the bound BR. An analysis of the BSA and SSA difference spectra (the spectrum of BR/SA/GS = 3/1/1 was subtracted from BR/SA = 3/1) definitely showed that the binding of GS crossed over the BR primary binding site on these proteins. The difference spectra for BSA and SSA showed the blocked binding site with the preferred M-stereoselectivity of BR, which, according to the specified preferences of the binding sites (Fig. 2), is the high-affinity binding site. On the basis of the specified preferences of the primary binding sites for BR (Fig. 2), we can conclude that GS blocked the high-affinity binding site.

The third group of the SAs studied, which included RSA and RbSA, showed a decrease of the intensity (42% for RbSA) and an inverted CD signal for RSA after GS addition (Fig. 5) at BR/SA = 3/1. The chirality of the blocked binding site indicated by difference spectra was identified as P-chirality, which is in agreement with the selectivity of the primary binding sites of these SAs (cf. Fig. 2.).

To interpret the observed chiroptical properties, the sequence composition of this site was analyzed (Fig. 6) and described in the SI.

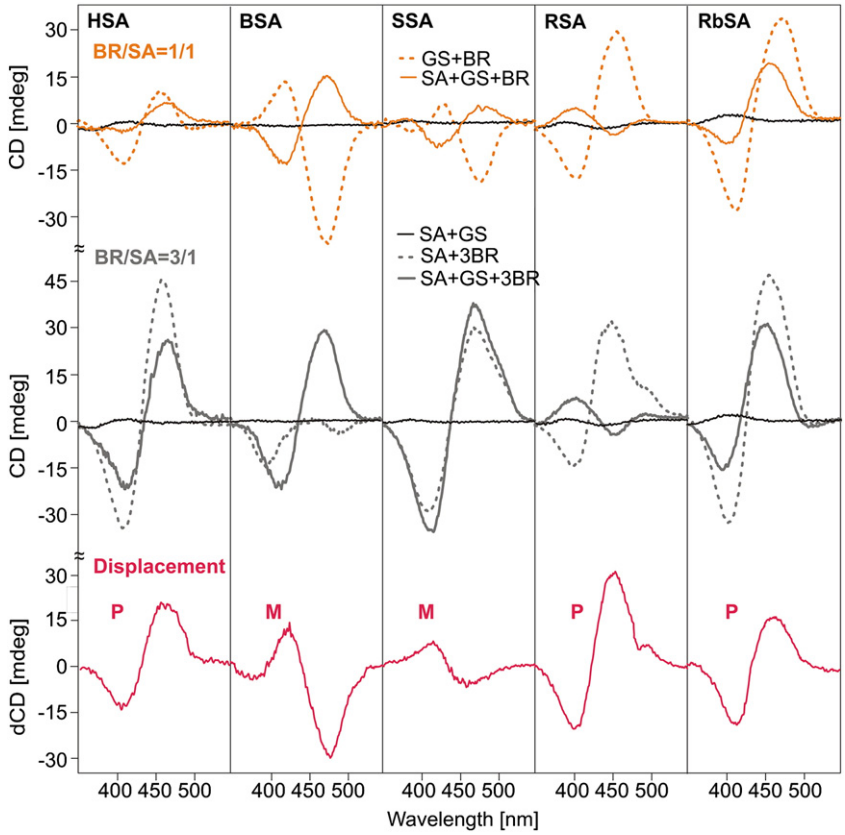

Fig. 5. The CD spectra of the BR complexes with human (HSA), bovine (BSA), sheep (SSA), rat (RSA) and rabbit (RbSA) serum albumins at the molar ratios BR/SA = 1/1 (orange) and BR/SA = 3/1 (gray) in the presence of gossypol (GS) at the molar ratio BR/SA/GS = 3/1/1 (full lines) and without GS (broken lines). The CD spectra of the BR–SA complexes without GS are in broken lines. The CD spectra of the SA–GS complexes at the molar ratio SA/GS = 1/1 are shown as black lines. The difference spectra dCD (red) were obtained when the spectrum of BR/SA/GS = 3/1/1 was subtracted from BR/SA = 3/1 and reflect the stereoselectivity of the BR-binding site blocked by GS.

In our simulation of the pigment binding to subdomain IIA in HSA, BSA and RbSA, we found that the arrangement of the Arg residues in the binding pocket determined the stereoselectivity of the bound pigment (see Fig. 6 and S4). The residue constitution of the pocket bottom (the neighborhood of Arg-257) for all the SAs studied has the same organization, so that the stereoselectivity of the pocket

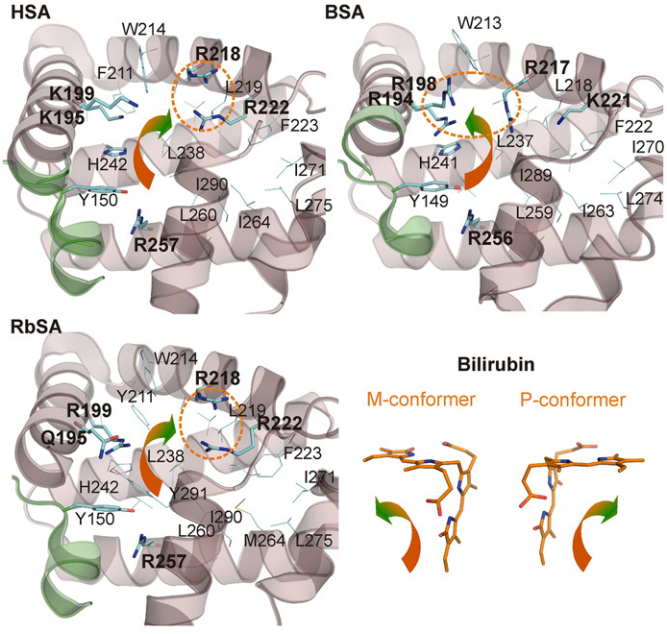

Residue	HSA	RbSA	RSA	Residue	BSA	SSA
	Albumin				Albumin	
195	K	Q	R	194	R	R
197	K	R	R	196	R	R
199	K	R	K	198	R	R
203	L	I	M	202	I	I
211	F	Y	F	210	L	L
214	W	W	W	213	W	W
218	R	R	R	217	R	R
219	L	L	M	218	L	L
222	R	R	R	221	K	K
223	F	F	F	222	F	F
234	L	I	L	233	L	I
235	V	V	A	234	V	V
238	L	L	V	237	L	L
241	V	V	I	240	V	V
242	H	H	H	241	H	H
257	R	R	R	256	R	R
260	L	L	L	259	L	L
264	I	M	M	263	I	I
271	I	I	I	270	I	L
275	L	L	L	274	L	L
290	I	I	L	289	I	L

Fig. 6. The spatial structure of the M- and P-helical conformers of BR, the structures of subdomains IIA for human (HSA), bovine (BSA) and rabbit (RbSA) serum albumins, and the amino-acid composition for human (HSA), rabbit (RbSA), rat (RSA), bovine (BSA) and sheep (SSA) serum albumins. The arrows show the chirality of the preferred BR conformer with respect to the location of the charged residues.

was driven by the organization of the polar residues on the opposite side of the pocket (see Fig. 6). HSA and RbSA contain the Arg-218/Arg-222 pair (the dotted circle in Fig. 6), which binds with the carboxyl groups of BR, and the bound pigment has adopted a P-conformation [2,4,5] as shown in Fig. 6. This is in agreement with the selectivity of BR bound on the HSA and RbSA primary sites (cf. Fig. 2), shown as positive couplets and assigned as P-conformers. In addition, it has been known from the crystallographic data for BSA that the localization of the charged residues within the pocket is different from that for HSA and RbSA (Fig. 6): While the first polar focal point at Arg-256 in BSA is similar to Arg-257 in HSA and RbSA, the second accessible Arg residue is situated on the other side of the binding pocket (Arg-194, Arg-198 and Arg-217). Consequently, one side of the BR molecule was bound on BSA at Arg-256 (analogical to Arg-257 in HSA and RbSA) and the other side of BR was bound in the Arg-194, Arg-198 and Arg-217 regions (the dotted circle in Fig. 6). As a result, the M-conformation of the bound BR was more favorable for BSA and SSA binding in the primary binding site as was demonstrated in Fig. 6. This is in accord with the observed negative couplet in the characteristics for the BR bound to the primary site in BSA and SSA (cf. Fig. 2). Taking all of the above data into account, we can hypothesize that subdomain IIA is a high-affinity binding site for BR on the proteins studied.

3.2.3. Subdomain IIIA

Subdomain IIIA was proposed as the third possible binding site. It is composed of all six helices of subdomain IIIA, which makes it topologically similar to the site in subdomain IIA [1,2,4]. It also comprises a largely pre-formed hydrophobic cavity with distinct polar features.

We suppose that subdomain IIIA is a secondary binding site. In our displacement experiments, Ibf was used as a marker for drug site II, which is located in subdomain IIIA [2–4]. It is known that Ibf selectively binds to this site with the binding constant $K_a = 2.7 \cdot 10^6\ M^{-1}$ [2]. The crystallographic structure of the Ibf–HSA complex has shown that the drugs were located deep inside the binding site and formed electrostatic interactions with the focal residue Arg-410. It has been known that Ibf can also bind in the secondary site located in subdomain IIB ($K_a = 1 \cdot 10^4\ M^{-1}$) [2,4,5]. In view of this fact, a threefold excess of the drug was used in our competition experiment. It should be noted that the CD signals of the Ibf–SA complexes did not interfere with or contribute to the CD spectrum of BR, because their absorption is in the UV region.

Fig. 7 shows the CD spectra of the studied complexes with and without Ibf. In the presence of Ibf, the changes in the CD spectra were observed when the final ratio of BR/HSA > 1. In the systems where BR is bound in the primary, high-affinity binding site, no significant changes in the CD pattern were observed. Significant differences were observed for the BR/SA = 3 and were caused by the displacement of BR from the secondary sites by Ibf. The difference spectra (the spectrum of BR/SA/Ibf = 3/1/3 was subtracted from BR/SA = 3/1) are also in agreement with our proposition: Fig. 7 shows that upon blocking by Ibf, BSA and SSA lost one bond per BR site with a P-preference (secondary site). The same site with the P-stereoselectivity for BR was blocked on HSA and RSA. A very pronounced and interesting effect was observed for RSA: at the ratio BR/RSA = 3/1, the inversion of the CD signal for the bound BR was observed when systems with and without Ibf were compared. This is in compliance with the supposition about the M-chirality of the bound pigment in the secondary site of RSA subdomain IB (cf. Fig. 4). Simultaneously, a weak decrease in the CD intensity of RbSA/BR = 3/1 after Ibf addition was observed.

Finally, these spectral and competition results are correlated with the structure of subdomain IIIA of the studied SAs (SI).

Our simulations of BR binding to subdomain IIIA are shown in Fig. 8. As the sequences of amino-acid residues in these domains are very similar for all studied SAs, we assume a similar stereoselectivity of this site for all of the SAs studied. We proposed that the bound BR adopted a P-helical conformation because of the orientation of the

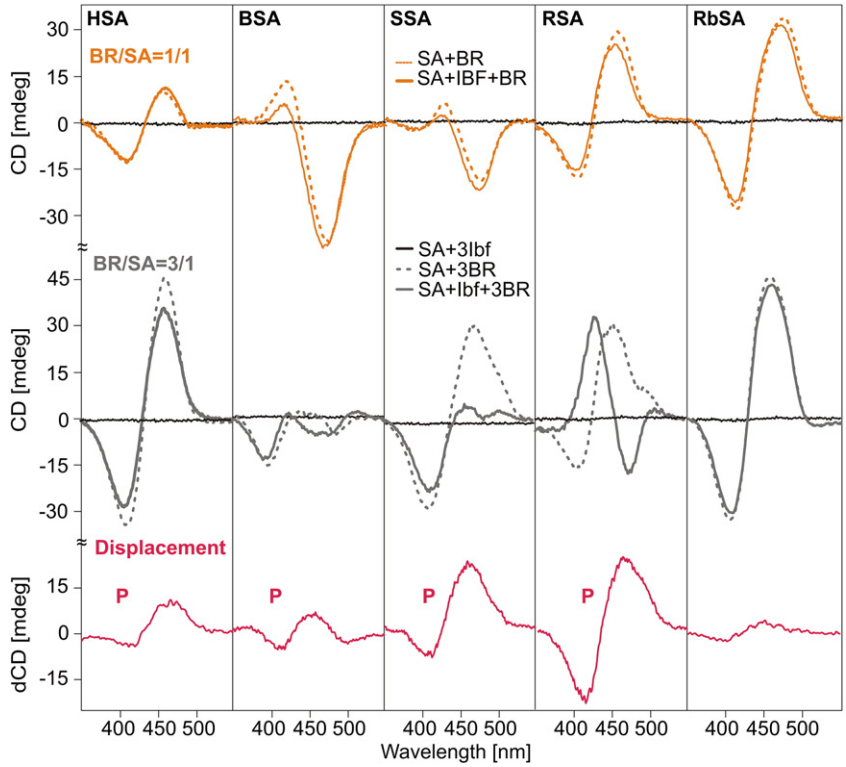

Fig. 7. The CD spectra of the Ibf complexes with human (HSA), bovine (BSA), sheep (SSA), rat (RSA) and rabbit (RbSA) serum albumins at the molar ratios Ibf/SA = 3/1 titrated by BR for the BR/SA/Ibf = 1/1/3 (orange) and 3/1/3 (gray). CD spectra of the BR–SA complexes without Ibf are in broken lines. The CD spectra of the Ibf–SA complexes at the molar ratio SA/Ibf = 1/3 are shown as black lines. The difference spectra dCD (red) were obtained when the spectrum of BR/SA/Ibf = 3/1/3 was subtracted from BR/SA = 3/1 and reflect the stereoselectivity of the BR-binding site blocked by Ibf.

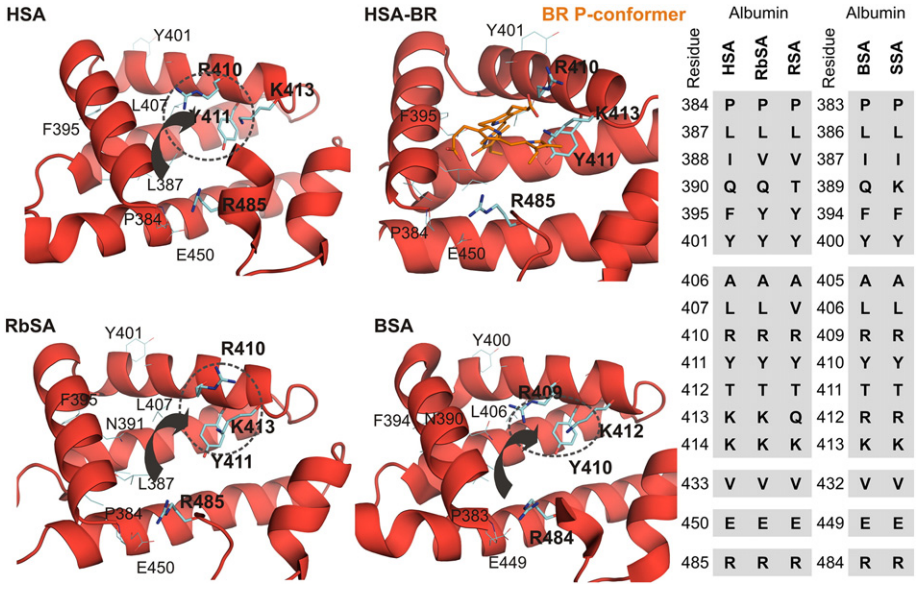

Residue	HSA	RbSA	RSA	Residue	BSA	SSA
384	P	P	P	383	P	P
387	L	L	L	386	L	L
388	I	V	V	387	I	I
390	Q	Q	T	389	Q	K
395	F	Y	Y	394	F	F
401	Y	Y	Y	400	Y	Y
406	A	A	A	405	A	A
407	L	L	V	406	L	L
410	R	R	R	409	R	R
411	Y	Y	Y	410	Y	Y
412	T	T	T	411	T	T
413	K	K	Q	412	R	R
414	K	K	K	413	K	K
433	V	V	V	432	V	V
450	E	E	E	449	E	E
485	R	R	R	484	R	R

Fig. 8. The spatial structure of the M- and P-helical conformers of BR, the structures of subdomains IIIA for human (HSA), bovine (BSA) and rabbit (RbSA) serum albumins, and the amino-acid composition for human (HSA), rabbit (RbSA), rat (RSA), bovine (BSA) and sheep (SSA) serum albumins. The arrows show the chirality of the preferred BR conformer with respect to the location of the charged residues.

charged pair Arg-410/Arg-485 and of the h1/h4 helices of HSA and Arg-409/Arg-484 in subdomain IIA for BSA, respectively.

The spectral effects accompanying titrations and the competition observed along with the analysis of amino-acid residues confirm our idea of the low-affinity binding site in subdomain IIIA. The summarized stereoselectivity of the BR-binding sites on the proteins studied is shown in Table 2.

4. Conclusions

Our results have proven the existence of three independent BR-binding sites in the structure of mammalian SAs. One high-affinity site (primary) and two secondary sites were analyzed in terms of their selective preference for the M- or P-helical conformers of BR.

We compared the total amounts of BR bound to HSA in the presence and absence of the marker ligands that can affect the capacity of SA to bind BR. Using selective markers for the three proposed binding sites (hemin, GS and Ibf), we confirmed the location of the high-affinity site (subdomain IIA) and of the secondary ones (subdomains IB and IIIA) and we specified their stereoselectivity. An addition of a competitor ligand to BR–HSA = 1/1 clearly caused a redistribution of the BR among the other sites. These data were indicative of the remarkable buffering capacity of albumin, consistent with many previous observations, and also suggested that drug binding does not necessarily affect the BR-binding capacity of albumin at typical BR/protein ratios in vivo, although it could affect binding affinities, like the blocking of the primary binding site provokes SA to bind the BR molecule in the secondary sites.

Table 2
The location, affinity and stereoselectivity of the BR-binding sites.

	Primary binding site (high affinity)	Secondary binding sites (low affinity)	
Protein	Subdomain IIA	Subdomain IB	Subdomain IIIA
HSA	P	P	P
BSA	M	P	P
SSA	M	P	P
RSA	P	M	P
RbSA	P	P	–[a]

[a] Cannot be proven by CD.

Additionally, the correlation between the stereoselectivity of the binding sites and the arrangement of the charged residues was made. On its basis, a simulation of the conformation of the bound BR in the proposed subdomains was performed. We are currently working on the selective step-by-step blocking of the binding sites for tetrapyrrolic compounds in order to provide their location and affinity.

Acknowledgments

The Czech Science Foundation (P206/11/0836) and the Specific University Research (MSMT No. 20/2013, A2_FCHI_2013_010) are gratefully acknowledged for financial support.

Appendix A. Supplementary data

Supplementary data to this article can be found online at http://dx.doi.org/10.1016/j.bpc.2013.06.004.

References

[1] X.M. He, D.C. Carter, Atomic structure and chemistry of human serum albumin, Nature 358 (1992) 209–215.
[2] T. Peters Jr., Serum Albumin, vol. 37, 1985, pp. 161–245.
[3] S. Curry, Lessons from the crystallographic analysis of small molecule binding to human serum albumin, Drug metabolism and pharmacokinetics 24 (2009) 342–357.
[4] J. Ghuman, P.A. Zunszain, I. Petitpas, A.A. Bhattacharya, M. Otagiri, S. Curry, Structural basis of the drug-binding specificity of human serum albumin, Journal of Molecular Biology 353 (2005) 38–52.
[5] U. Kragh-Hansen, V.T.G. Chuang, M. Otagiri, Practical aspects of the ligand-binding and enzymatic properties of human serum albumin, Biological and Pharmaceutical Bulletin 25 (2002) 695–704.
[6] D.C. Carter, J.X. Ho, Structure of serum albumin, Advances in Protein Chemistry 45 (1994) 153–203.
[7] L. Vítek, J. Donald Ostrow, Bilirubin chemistry and metabolism; harmful and protective aspects, Current Pharmaceutical Design 15 (2009) 2869–2883.
[8] S.E. Boiadjiev, D.A. Lightner, Optical activity and stereochemistry of linear oligopyrroles and bile pigments, Tetrahedron-Asymmetry 10 (1999) 607–655.
[9] G. Le Bas, A. Allegret, Y. Mauguen, C. de Rango, M. Bailly, The structure of triclinic bilirubin chloroform–methanol solvate, Acta Crystallographica. Section B 36 (1980) 3007–3011.
[10] D.A. Lightner, M. Reisinger, G.L. Landen, On the structure of albumin-bound bilirubin. Selective binding of intramolecularly hydrogen-bonded conformational enantiomers, Journal of Biological Chemistry 261 (1986) 6034–6038.
[11] I. Goncharova, M. Urbanova, Stereoselective bile pigment binding to polypeptides and albumins: a circular dichroism study, Analytical and Bioanalytical Chemistry 392 (2008) 1355–1365.

[12] I. Goncharova, M. Urbanova, Bile pigment complexes with cyclodextrins: electronic and vibrational circular dichroism study, Tetrahedron-Asymmetry 18 (2007) 2061–2068.
[13] I. Goncharova, S. Orlov, M. Urbanová, Chiroptical properties of bilirubin-serum albumin binding sites, Chirality 25 (2013) 257–263.
[14] R. Brodersen, Bilirubin transport in the newborn infant, reviewed with relation to kernicterus, Journal of Pediatrics 96 (1980) 349–356.
[15] A. Knudsen, A.O. Pedersen, R. Brodersen, Spectroscopic properties of bilirubin-human serum albumin complexes: a stoichiometric analysis, Archives of Biochemistry and Biophysics 244 (1986) 273–284.
[16] J. Jacobsen, R. Brodersen, Albumin-bilirubin binding mechanism. Kinetic and spectroscopic studies of binding of bilirubin and xanthobilirubic acid to human serum albumin, Journal of Biological Chemistry 258 (1983) 6319–6326.
[17] R. Brodersen, L. Funding, A.O. Pedersen, H. Röigaard-Petersen, Binding of bilirubin to low-affinity sites of human serum albumin in vitro followed by co-crystallization, Scandinavian Journal of Clinical and Laboratory Investigation 29 (1972) 433–446.
[18] R. Brodersen, Binding of bilirubin to albumin, CRC Critical Reviews in Clinical Laboratory Sciences 11 (1980) 305–399.
[19] P.A. Zunszain, J. Ghuman, A.F. McDonagh, S. Curry, Crystallographic analysis of human serum albumin complexed with 4Z,15E-bilirubin-IXα, Journal of Molecular Biology 381 (2008) 394–406.
[20] C.E. Petersen, C.E. Ha, K. Harohalli, J.B. Feix, N.V. Bhagavan, A dynamic model for bilirubin binding to human serum albumin, Journal of Biological Chemistry 275 (2000) 20985–20995.
[21] R.V. Person, B.R. Peterson, D.A. Lightner, Bilirubin conformational analysis and circular dichroism, Journal of the American Chemical Society 116 (1994) 42–59.
[22] C.E. Petersen, C.E. Ha, S. Curry, N.V. Bhagavan, Probing the structure of the warfarin-binding site on human serum albumin using site-directed mutagenesis, Proteins 47 (2002) 116–125.
[23] M. Pistolozzi, C. Bertucci, Species-dependent stereoselective drug binding to albumin: a circular dichroism study, Chirality 20 (2008) 552–558.
[24] C.N. Pace, F. Vajdos, L. Fee, G. Grimsley, T. Gray, How to measure and predict the molar absorption coefficient of a protein, Protein Science 4 (1995) 2411–2423.
[25] K.A. Majorek, P.J. Porebski, A. Dayal, M.D. Zimmerman, K. Jablonska, A.J. Stewart, M. Chruszcz, W. Minor, Structural and immunologic characterization of bovine, horse, and rabbit serum albumins, Molecular Immunology 52 (2012) 174–182.
[26] D. Seeliger, B.L. De Groot, Ligand docking and binding site analysis with PyMOL and Autodock/Vina, Journal of Computer-Aided Molecular Design 24 (2010) 417–422.
[27] M.J. Geisow, G.H. Beaven, Physical and binding properties of large fragments of human serum albumin, Biochemistry Journal 163 (1977) 477–484.
[28] A. Minomo, Y. Ishima, U. Kragh-Hansen, V.T.G. Chuang, M. Uchida, K. Taguchi, H. Watanabe, T. Maruyama, H. Morioka, M. Otagiri, Biological characteristics of two lysines on human serum albumin in the high-affinity binding of 4Z,15Z-bilirubin-IXα revealed by phage display, FEBS Journal 278 (2011) 4100–4111.
[29] J. Wang, T.T. Ndou, I.M. Warner, C.P. Pau, Spectroscopic analysis and drug-binding studies of the CNBr fragments of human serum albumin, Talanta 40 (1993) 557–563.
[30] R.E. Royer, D.L. Vander Jagt, Gossypol binds to a high-affinity binding site on human serum albumin, FEBS Letters 157 (1983) 28–30.
[31] I. Petitpas, A.A. Bhattacharya, S. Twine, M. East, S. Curry, Crystal structure analysis of warfarin binding to human serum albumin — anatomy of drug site I, Journal of Biological Chemistry 276 (2001) 22804–22809.
[32] R.G. Reed, R.C. Feldhoff, O.L. Clute, T. Peters Jr., Fragments of bovine serum albumin produced by limited proteolysis. Conformation and ligand binding, Biochemistry-Us 14 (1975) 4578–4583.
[33] R. Brodersen, B. Friishansen, L. Stern, Drug-induced displacement of bilirubin from albumin in the newborn, Developmental pharmacology and therapeutics 6 (1983) 217–229.